

SCIENTIFIC REPORTS



OPEN

Nanofiber network with adjustable nanostructure controlled by PVP content for an excellent microwave absorption

Jing Lv^{1,2}, Weihua Gu², Xiaoqing Cui², Sisi Dai², Baoshan Zhang¹ & Guangbin Ji²

Carbon nanofibers were widely utilized to improve microwave absorption properties since they are a promising lightweight candidate. Adjustable conductive nanostructures of carbon nanofibers were synthesized by electrospinning technique. The conductive network is controlled by the polyvinyl pyrrolidone (PVP) content due to the special hygroscopicity of PVP. The increased adhesive contacts of nanofibers provide more transmission paths for electrons to reduce the effect of air dielectric. Satisfactorily, the carbon nanofibers that carbonized from the polyacrylonitrile (PAN) and PVP (the mass ratio is 6:4) show excellent microwave absorption performance. The minimum reflection loss (RL) value is -51.3 dB at 15.2 GHz and the maximum effective absorption frequency width (< -10 dB) is 5.1 GHz with the matching thickness of only 1.8 mm. Thereby, we believe that this research may offer an effective way to synthesize lightweight carbon nanofibers microwave absorbers.

In modern society, electromagnetic (EM) absorbers have become an indispensable part of information equipment, which can reduce the harm to the surroundings and the humans. The principle of EM absorbers is making microwave transform into other types of energy to attenuate EM wave^{1–3}. Traditional microwave absorption materials like metal as well as alloys, ferrites and all varieties of these composites with strong microwave absorption abilities and broad effective frequency width develop rapidly. However, it is also significant for actual demand to reduce the density and weight of microwave absorbers at the same time^{4–6}.

As famous lightweight materials, carbon nanomaterials have been achieved tremendous attention. Various classes of carbon nanoparticles such as carbon nanotubes, carbon cloths and so on are of many wonderful characters such as large areas, low cost, good stability and great electrical conductivity^{7–10}. Thereby, carbon nanomaterials are quite befitting for EM wave absorption field^{11,12}. Among numerous carbon nanomaterials, carbon nanofibers are of huge interest for EM wave absorption due to their one-dimensional nanostructure that can form conductive network^{13–15}. For instance, Liu *et al.* successfully fabricated a kind of helical CNFs coated-carbon fibers through catalytic chemical vapor deposition. The minimum RL value was -32 dB at 9.0 GHz and the widest effective frequency width was 9.8 GHz with only 15% filler ratio¹⁶. Porous carbon nanotubes decorated carbon nanofibers were also achieved with the minimum RL value of -44.5 dB at 10.7 GHz as well as the broad effective frequency width of 7.1 GHz¹⁷. Chu *et al.* compared the microwave absorption abilities of different diameters, they believed that complex permittivity improved along with the decreasing diameters since it contributed to the conductive network¹⁸. Based on their researches, we can discover that the microwave absorption performance closely depends on their design of one-dimensional nanostructures on carbon nanofibers. In principle, morphology change of carbon nanofibers could dramatically influence the transferring path of the electrons as well as the construction of the conductive network¹⁹. Accordingly, the permittivity and polarization process would be controlled in the range of testing frequency artificially. Furthermore, electrospinning fiber technique can be used accurately to obtain diversiform nanofibers, which is a good choice to synthesize carbon nanofibers^{20,21}.

In this paper, we added PVP as a structural adjuster to modify PAN based carbon nanofibers by changing the PVP content, followed by electrospinning and next annealing process. PVP, as a high-molecular compound, it is liable to dissolve in water. In addition, the more average molecular weight of PVP, the more chance of it to be

¹School of Electronic Science and Engineering, Nanjing University, Nanjing, 210093, P.R. China. ²College of Materials Science and Technology, Nanjing University of Aeronautics and Astronautics, Nanjing, 210016, P.R. China. Correspondence and requests for materials should be addressed to B.Z. (email: bszhang@nju.edu.cn)



Figure 1. Synthesis schematic diagram of carbon nanofibers with adjustable nanostructure.

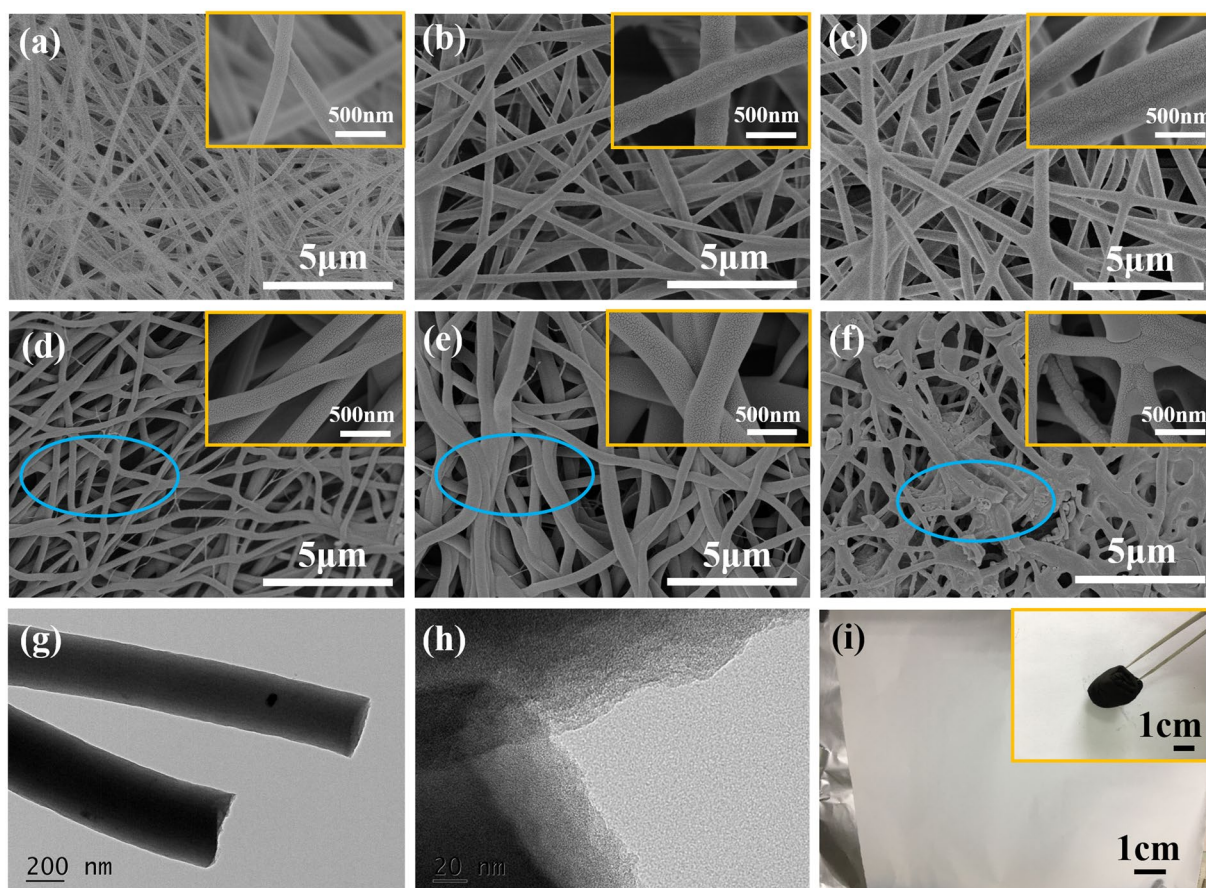


Figure 2. SEM images of (a) PAN/PVP-7/3 (b) PAN/PVP-6/4 (c) PAN/PVP-5/5 (d) PVP (214) (e) PVP (333) (f) PVP (500) samples, Inserts are magnified images; (g,h) TEM images of PVP (333) sample; (i) physical photo of PAN/PVP-6/4 sample, Insert is the physical photo of PVP (333) sample.

agglutinating²². Considering with these intrinsic qualities of PVP, we easily gain nanofiber network with adjustable nanostructure controlled by PVP content. Gratifyingly, the microwave absorption performance is enhanced, too. For the carbon nanofibers carbonized from the PAN and PVP (the mass ratio is 6:4 and the filler ratio is 20%), the RL value is -51.3 dB at 15.2 GHz and the maximum effective absorption frequency width (< -10 dB) is 5.1 GHz with only 1.8 mm. This work provides a novel strategy to build the conductive network of carbon nanofibers through adjusting the content of PVP, which may be impulse the development of the lightweight microwave absorbers.

Results

Figure 1 is the entire synthesis schematic diagram of our nanofibers conductive network. The precursor solution of PAN and PVP was transformed into nanofibers via a representative electrospinning technology. After being treated at 800 °C for 3 h under N_2 atmosphere inside tube furnace, carbon nanofibers with adjustable nanostructure were finally fabricated.

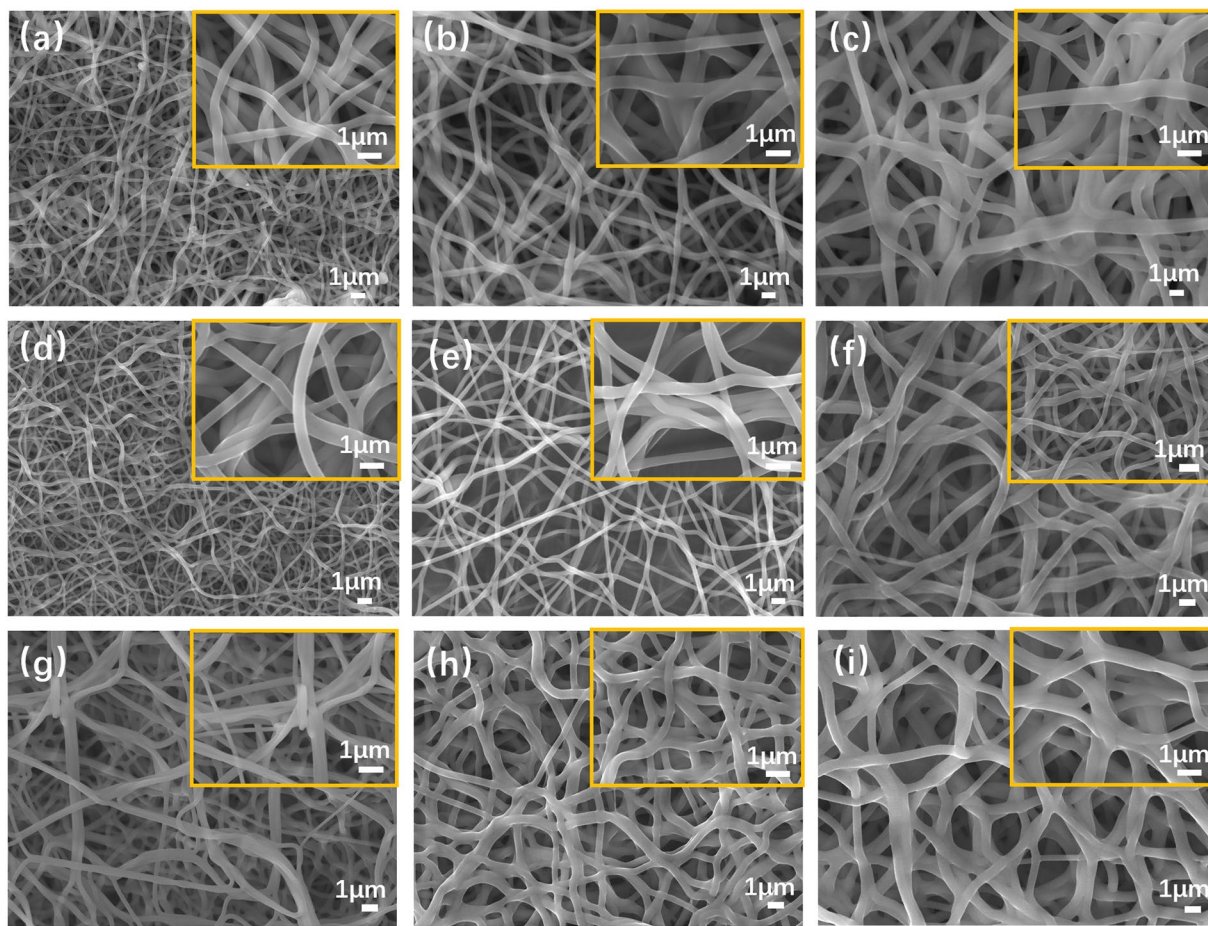


Figure 3. SEM images of (a) PVP (214–200) (b) PVP (333–200) (c) PVP (500–200) (d) PVP (214–400) (e) PVP (333–400) (f) PVP (500–400) (g) PVP (214–600) (h) PVP (333–600) (i) PVP (500–600) samples. Inserts are magnified images.

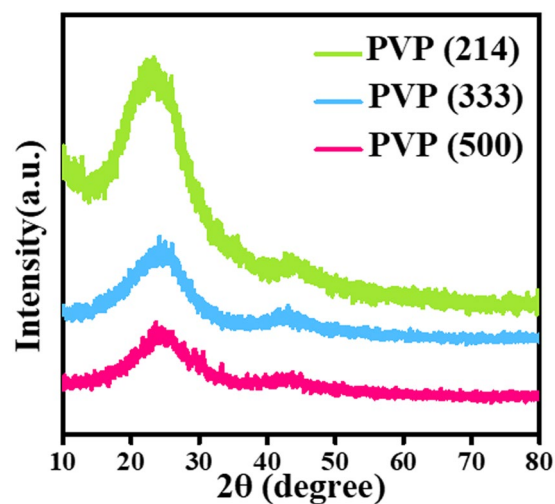


Figure 4. XRD patterns of PVP (214), PVP (333) and PVP (500).

Detailed nanostructures of different nanofibers are detected using SEM and TEM methods. Obviously, nanofibers of PAN/PVP samples show typical one-dimensional morphology of electrospun fibers in Fig. 2(a–c). There surfaces are smooth. In addition, we can easily see that the nanofibers become more and more thicker since the quality of PAN is constant and the quality of PVP is larger. The average diameters of PAN/PVP-7/3 sample, PAN/PVP-6/4 sample and PAN/PVP-5/5 sample are 167 nm, 277 nm and 444 nm, respectively. After calcined at 800 °C

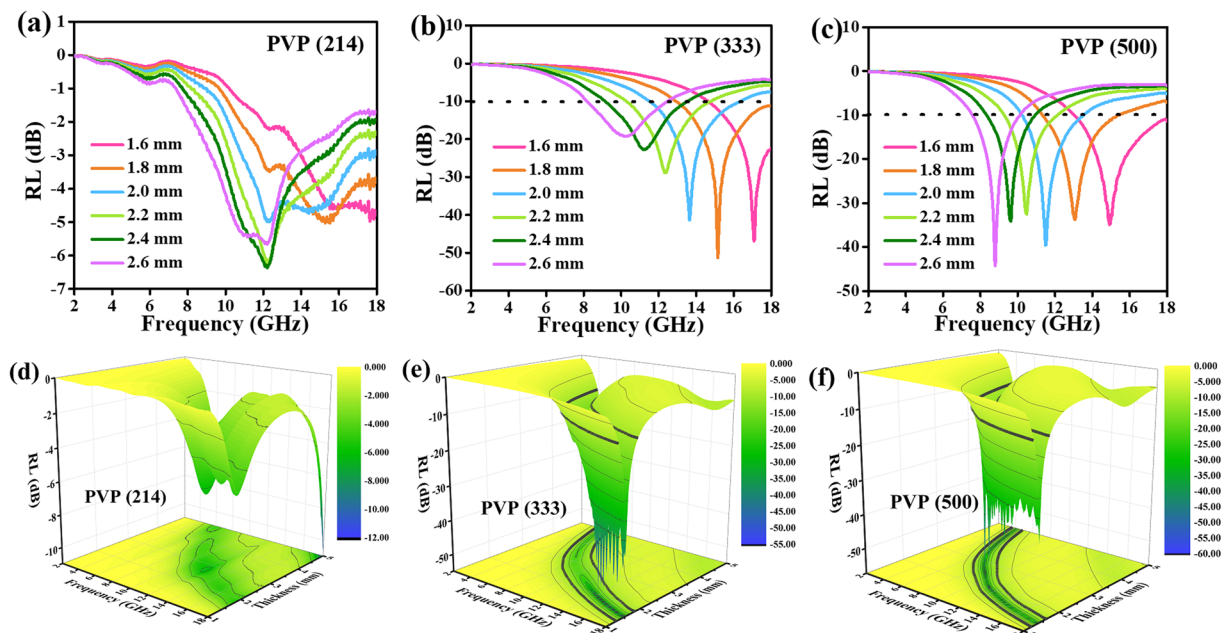


Figure 5. RL values of (a) PVP (214) (b) PVP (333) and (c) PVP (500) samples with matching thickness of 1.6 mm, 1.8 mm, 2.0 mm, 2.2 mm, 2.4 mm and 2.6 mm; 3D RL plots of (d) PVP (214) (e) PVP (333) (f) PVP (500) samples in the range of 2–18 GHz.

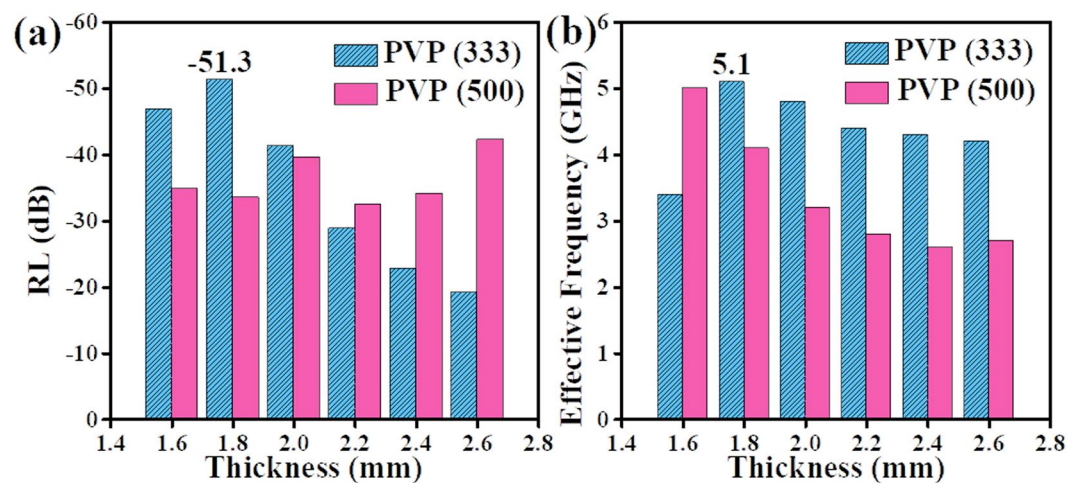


Figure 6. (a) RL peak values and (b) f_E peak values of PVP (333) sample and PVP (500) sample with different thickness of 1.6 mm, 1.8 mm, 2.0 mm, 2.2 mm, 2.4 mm and 2.6 mm.

under N_2 atmosphere, it can be seen that some of nanofibers are bent and bonded in Fig. 2(d–f). Notably, this phenomenon is relatively clearer with the increasing content of PVP. Due to the strong hygroscopicity of PVP, the solvent doesn't volatilize very well so that the nanofibers change into a sticky one. However, nanofibers of PVP (500) sample present a fracture situation. It is very difficult to identify the one-dimensional nanofibers in Fig. 1(f). Moreover, Fig. 2(g,h) displays the TEM pictures of PVP (333) sample. It should be noticed that there is typical carbon margin in Fig. 2(h). Also, physical photos of the white PAN/PVP-6/4 sample and the black PVP (333) sample are provided in Fig. 2(i).

The PAN/PVP nanofibers were also heated at 200 °C, 400 °C and 600 °C. As can be seen from Fig. 3, all of these samples present a curved one-dimensional nanofibers morphology. The nanofibers are getting thicker with the increasing content of PVP. Besides, the fusing phenomenon becomes serious when we added more PVP.

Figure 4 offers us with the similar XRD patterns of PVP (214) sample, PVP (333) sample and PVP (500) sample. Obviously, we have successfully achieved amorphous carbon nanofibers. No impurities can be detected.

The RL values of different carbon nanofibers are provided in Fig. 5(a–f) using the following formulas^{23–25}:

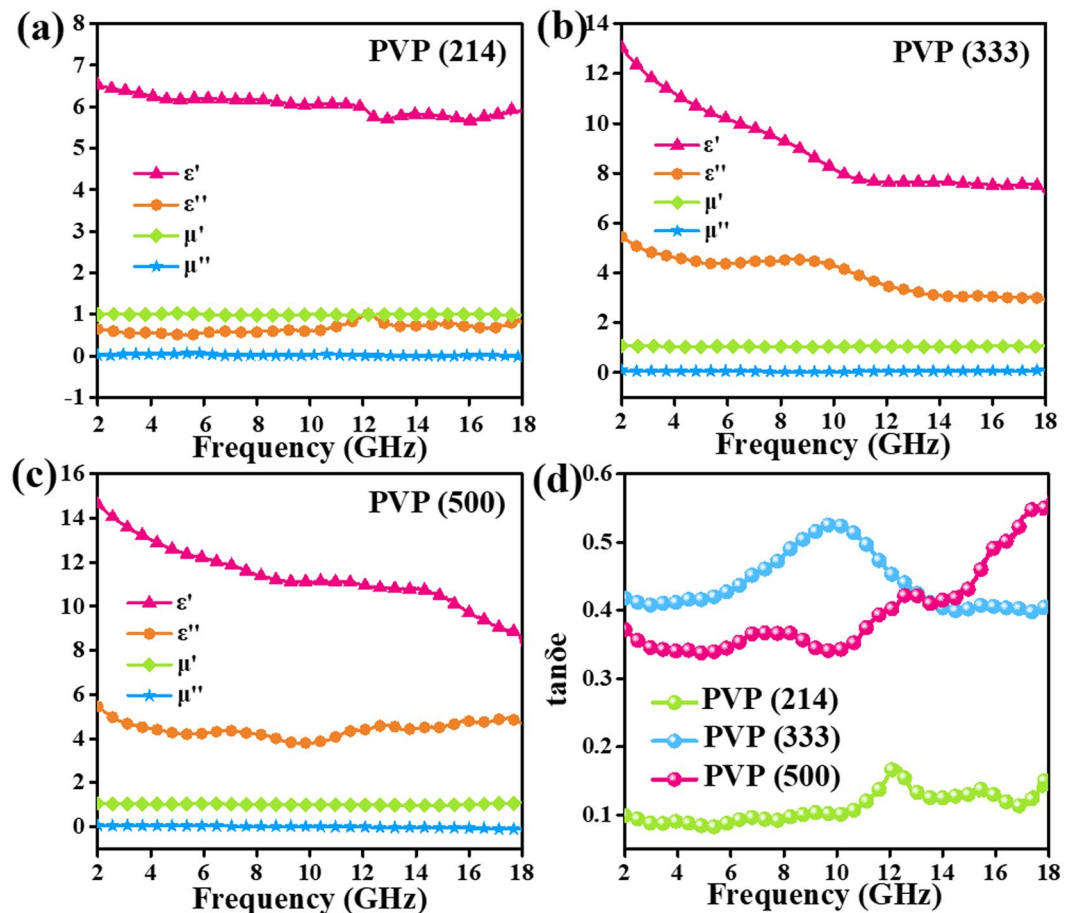


Figure 7. Frequency dependence on electromagnetic parameters of (a) PVP (214) (b) PVP (333) and (c) PVP (500) samples in the range of 2–18 GHz.

$$RL = 20 \log_{10} |(Z_{in} - Z_0)/(Z_{in} + Z_0)| \quad (1)$$

$$Z_{in} = \sqrt{(\mu_r/\varepsilon_r)} \tanh \left[j \left(\frac{2\pi}{c} \right) f d \sqrt{(\mu_r \varepsilon_r)} \right] \quad (2)$$

where Z_{in} is the input impedance, Z_0 is the impedance of free space, f is the frequency, d and c represent the thickness and the velocity of light, respectively. When the thickness increases, the RL values shifts to lower frequency, indicating that EM wave absorption frequency and the thickness of absorbers can be modulated. Among PVP (214), PVP (333) and PVP (500) samples, PVP (214) sample shows the poorest microwave absorption abilities. Different microwave absorption performances have something to do with the content of PVP. As the RL values below -10 dB, effective microwave absorbers will make 90% microwave attenuated²⁶. Thereby, when matching thickness are 1.6 mm, 1.8 mm, 2.0 mm, 2.2 mm, 2.4 mm and 2.6 mm, RL values of PVP (333) sample and PVP (500) sample can meet the actual application requirements. That is, for PVP (333) sample, the minimum RL value is -51.3 dB at 15.2 GHz and the maximum effective absorption frequency width ($f_E, < -10$ dB) is 5.1 GHz both with 1.8 mm of thickness. Moreover, for PVP (500) sample, the minimum RL value is -44.3 dB at 8.8 GHz with 2.6 mm as well as the maximum effective absorption frequency width is 5.0 GHz with only 1.6 mm. To compare the microwave absorption performance of PVP (333) sample and PVP (500) sample, RL peak values and f_E peak values of PVP (333) and PVP (500) with different thickness are given in Fig. 6(a,b). As seen in Fig. 6, PVP (333) sample has more boarder effective frequency width while the microwave absorption ability of PVP (500) sample is stronger.

The electromagnetic parameters (complex permittivity: $\varepsilon = \varepsilon' - j\varepsilon''$; the complex permeability: $\mu = \mu' - j\mu''$) of carbon nanofibers are tested by a network analyzer. Herein, magnetic properties of carbon nanofibers can be neglected since the dielectric loss more critical. Obviously, permittivity shows a sustainable growth with the increasing content of PVP. The ε' of PVP (214) sample is the lowest among these carbon nanofibers. The ε' of PVP (333) sample is from 13.0 to 7.2 while PVP (500) sample descends from 14.6 to 8.2. The ε'' values of PVP (333) sample and PVP (500) sample are higher than that of PVP (214) sample. In Fig. 7, some small fluctuations of ε'' curves arise from the multiple nature resonances. According to pervious reports, it was found that the

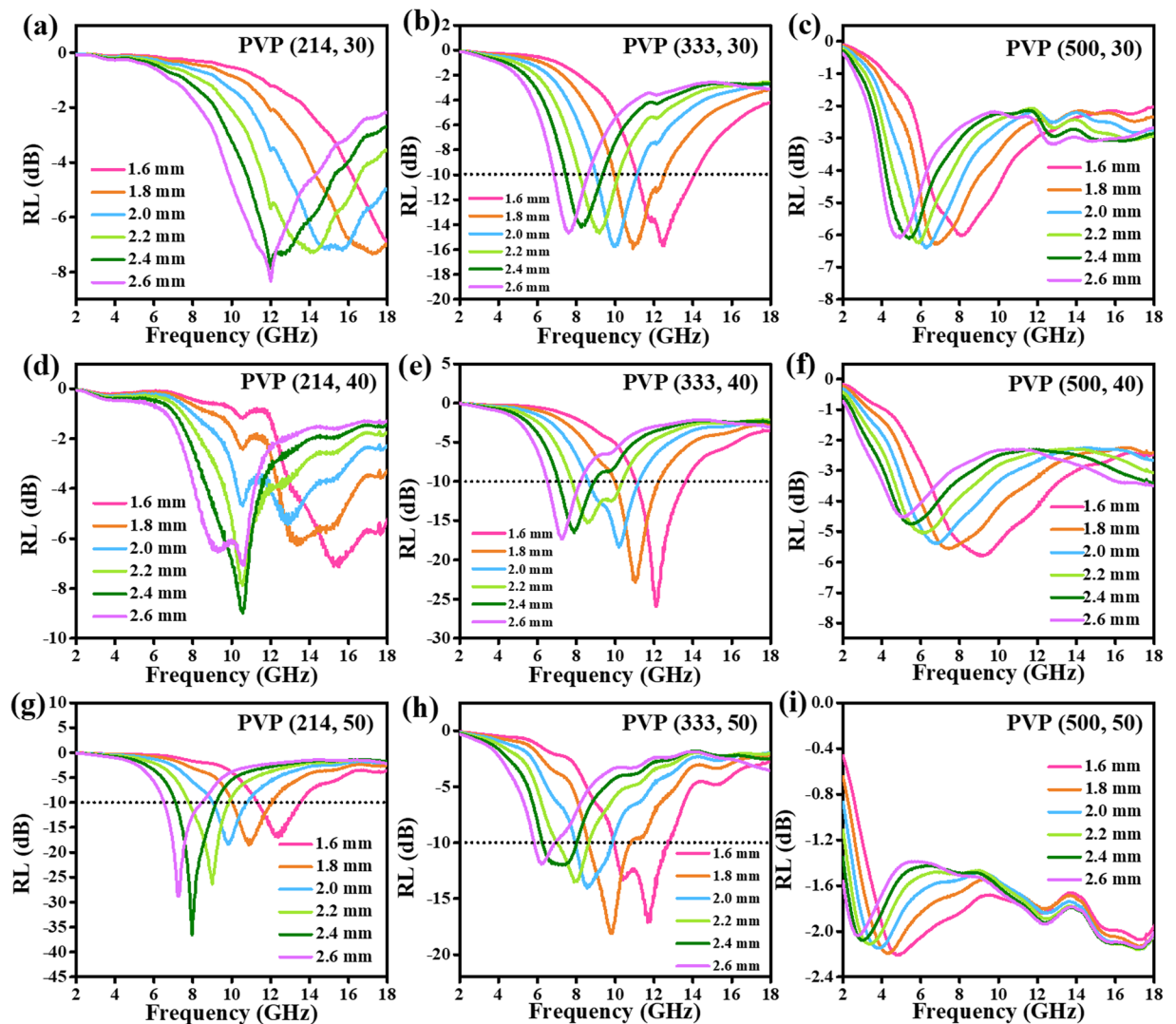


Figure 8. RL values of (a) PVP (214, 30) (b) PVP (333, 30) (c) PVP (500, 30) (d) PVP (214, 40) (e) PVP (333, 40) (f) PVP (500, 40) (g) PVP (214, 50) (h) PVP (333, 50) and (i) PVP (500, 50) in range of the 2–18 GHz.

complex permittivity would improve with the increasing average diameters of the PAN based carbon nanofibers¹⁸. Nevertheless, our nanofibers do not suit this situation. This phenomenon may refer to their special adhesive nanostructures. Namely, average diameters could not be the main reason that effects the complex permittivity. As we all know, if there are some gaps between nanofibers, air will reduce the dielectric of nanofibers, bringing about lower permittivity values. Therefore, the adhesive carbon nanofibers would be the dominant reason that increases the dielectric constant. Thanks to the function of PVP, the more contact carbon nanofibers, the electrical conductivity is higher. As studied by other groups, dielectric loss can be caused by conductive loss as well as by polarization loss involved in the relaxation process²⁷. Moreover, different polarization process including ionic polarization, electronic polarization and dipole polarization can be considered in this cause²⁸. However, ionic polarization and electronic polarization always happen at high frequency such as 10^3 – 10^6 GHz, dipole polarization should be the main reason that leads to the polarization process. Using the Eq. (3), dielectric loss degree can be evaluated in Fig. 7(d)^{29–31}:

$$\tan \delta_e = \varepsilon''/\varepsilon' \quad (3)$$

The results manifest that the dielectric loss tangent of PVP (214) sample is around 0.1. The dielectric loss tangent curve of PVP (333) sample show a rising trend followed by a drop condition. PVP (500) sample show a raising trend. So, we suggest that both PVP (333) sample and PVP (500) are of higher dielectric loss.

The RL values and frequency dependence on electromagnetic parameters of different sample filler ratios are displayed in Figs 8 and 9. Accordingly, the permittivity goes up with the increasing sample filler ratio. When the sample filler ratios are 30% and 40%, the microwave absorption abilities of PVP (333) sample are much better than that of other two samples. Interestingly, RL values decreases with the increasing content of PVP when the

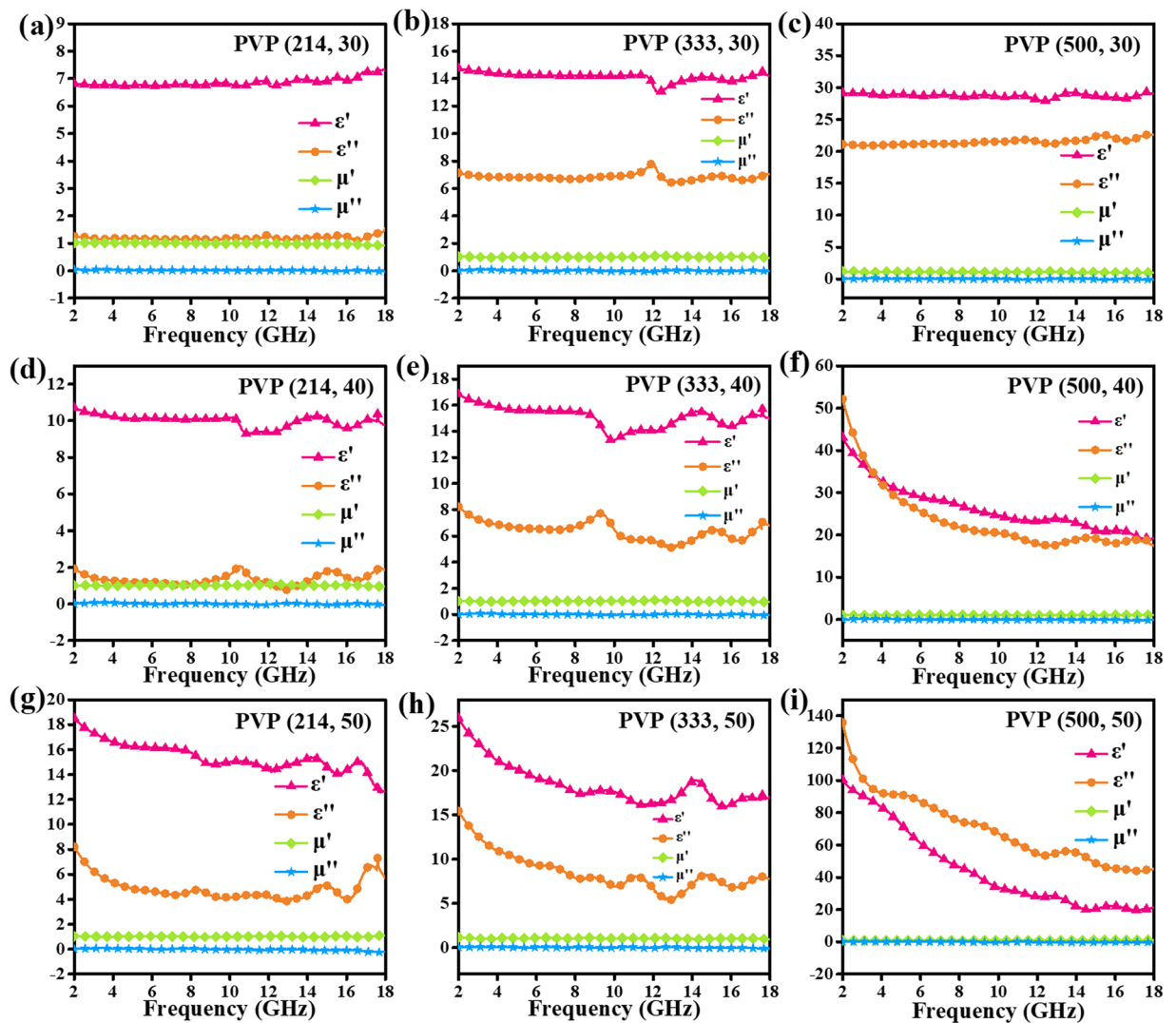


Figure 9. Frequency dependence on electromagnetic parameters of (a) PVP (214, 30) (b) PVP (333, 30) (c) PVP (500, 30) (d) PVP (214, 40) (e) PVP (333, 40) (f) PVP (500, 40) (g) PVP (214, 50) (h) PVP (333, 50) and (i) PVP (500, 50).

sample filler ratio is 50%. Particularly, PVP (214) shows the minimum RL value of -36.5 dB at 8.0 GHz with the thickness of 2.4 mm.

Impedance matching is an important factor to the microwave absorbers. If the nanofibers are of good impedance matching properties, more microwave will go into the nanofibers and will be attenuated^{32,33}. To synthesize a satisfactory microwave absorber, it is the key to improve the microwave absorption performance or board the effective frequency width. Figure 10 gives the 3D representation of $|Z_{in}/Z_0|$ values of PVP (214), PVP (333) and PVP (500) samples. Obviously, PVP (214) sample owns the most inferior impedance matching properties. For PVP (333) sample, the values of $|Z_{in}/Z_0|$ are almost near to 1, so the effective frequency widths of PVP (333) sample are boarder than PVP (214) sample and PVP (500) sample. And for PVP (500) sample, the values of $|Z_{in}/Z_0|$ can be 1, we obtain the strongest microwave absorption abilities from PVP (500) sample with 2.2 mm, 2.4 mm and 2.6 mm. These results accord to the analysis of Fig. 6. Taken the matching thickness of 1.6 mm and 1.8 mm as examples, it is pleased that the $|Z_{in}/Z_0|$ values of PVP (333) sample and PVP (500) sample are around 1, the RL values are meet the requirements of -10 dB. Particularly, PVP (333) sample gets the strongest microwave absorption abilities and the broadest effective frequency width with the thickness of 1.8 mm.

Conductive networks successfully are changed by different content of PVP. To further compared the conductivity of different content of PVP based carbon nanofibers. The conductivity values are evaluated using on the following formula²:

$$\sigma_{AC} = \varepsilon_0 \varepsilon'' \omega = \varepsilon_0 \varepsilon'' 2\pi f \quad (4)$$

$$\varepsilon_0 = 10^{(-9)/36\pi} \quad (5)$$

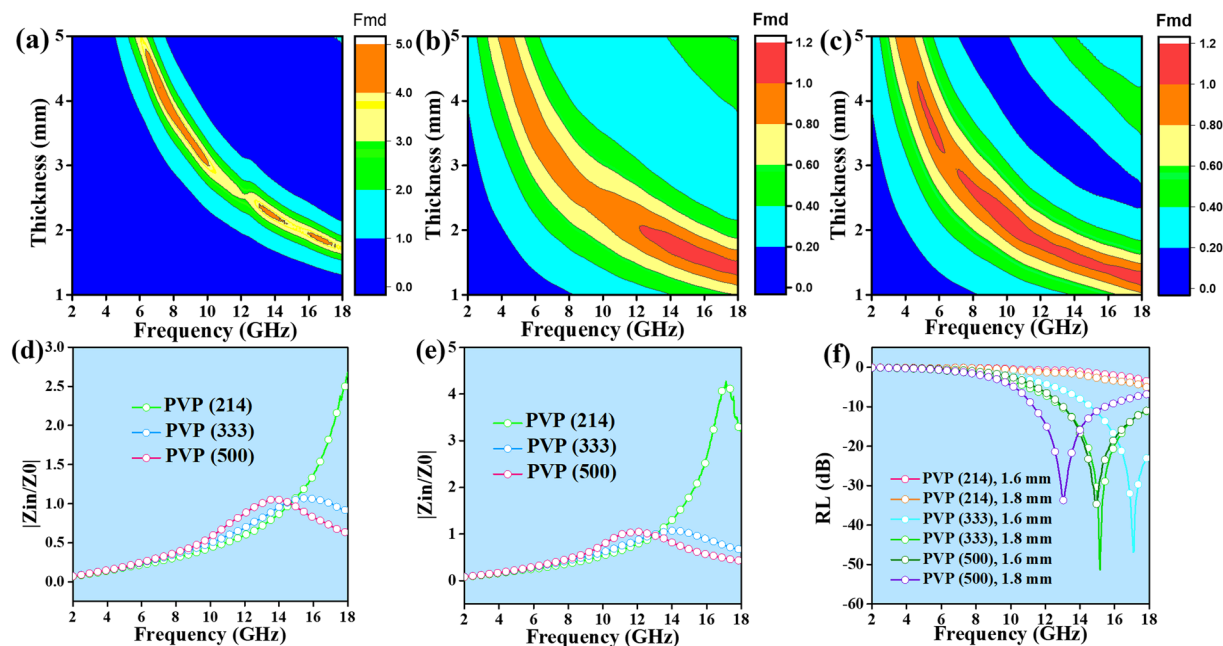


Figure 10. 3D representation of $|Z_{in}/Z_0|$ values of (a) PVP (214) (b) PVP (333) (c) PVP (500) samples; $|Z_{in}/Z_0|$ values of PVP (214), PVP (333) and PVP (500) samples with the thickness of (d) 1.6 mm (e) 1.8 mm and (f) RL values of PVP (214), PVP (333) and PVP (500) samples with the matching thickness of 1.6 mm and 1.8 mm.

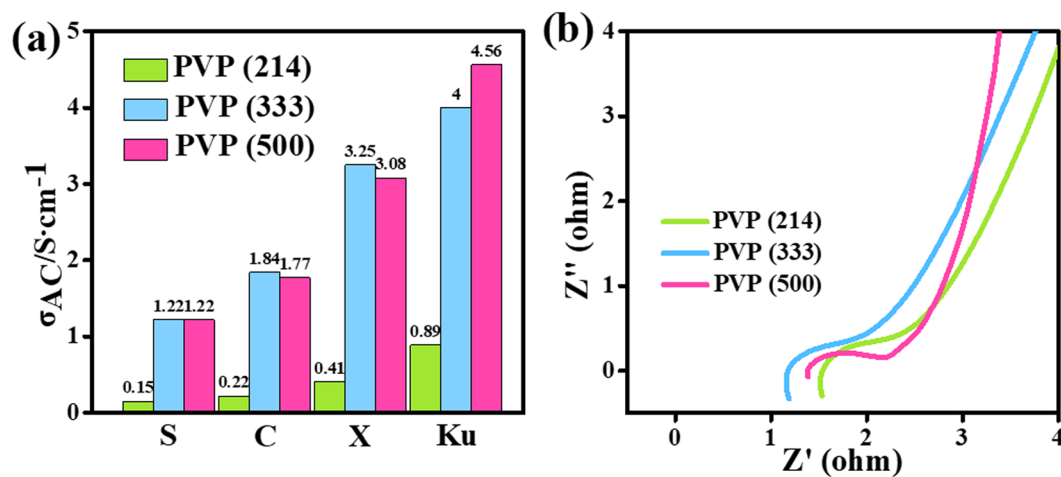


Figure 11. (a) Average conductivity values of PVP (214), PVP (333), and PVP (500) samples in S, C, X and Ku band; (b) Nyquist plot of PVP (214), PVP (333) and PVP (500).

In Fig. 11, PVP (214) sample shows the lowest average conductivity while the average conductivities of PVP (333) sample and PVP (500) can be greatly improved at S, C, X and Ku frequency range with the increasing content of PVP. The electronic impedance spectrum (EIS) for PVP (214), PVP (333) and PVP (500) were measured to evaluate their conductivity. As can be seen in the Nyquist plot in Fig. 11(b), the theoretical prediction of electrical conductivity in the following order PVP (214) < PVP (333) < PVP (500), indicating the higher conductivity with the increasing content of PVP. In this case, more contact positions of nanofibers will make electrons have multiple paths to transfer, which creates the increased conductivity. The carbon conductive network is fabricated simultaneously.

Table 1 gives some data of similar carbon nanofibers about their microwave absorption performance. In Table 1, we can easily conclude that all kinds of carbon nanofibers show enhanced microwave absorption abilities. Compared with carbon fibers that heap up one by one, nanofibers with some bonded places are more beneficial to make electrons transfer. When this type of carbon nanofiber is put in EM field, electron is likely to transfer with many paths. Hence, among these different carbon nanofibers, our adjustable shaped carbon nanofibers display the minimum RL value and broader effective bandwidth with the thinnest thickness, which implies that it is very potential to be used as lightweight microwave absorber.

Sample	RL _{mix} (dB)	Thickness (mm)	Filler loadings (wt%)	Effective bandwidth (< -10 dB)	Ref.
Hollow CNF	-23.0	3.0	33	2.3	18
Conductive nanocomposite fibers	-5.9	2.0	—	—	34
Porous-carbon-nanotube decorated CNF	-44.5	2.0	20	5.2	17
Carbon nanofiber/epoxy	-34.0	2.1	8	3.6	35
Porous CNF	-31.0	2.3	6	—	11
CNF with adjustable shape	-51.3	1.8	20	5.1	This work

Table 1. Comparison of some similar nanofibers on their microwave absorption properties.

Conclusion

Carbon nanofibers with adjustable nanostructure were gained by electrospinning method. When calcined at the same temperature (800 °C), the PVP content could be the main reason that influence the microwave absorption abilities. The increased adhesive contacts of nanofibers create the more paths for electrons to transfer and can reduce the effect of air dielectric. Furthermore, appropriate impedance matching is also responsible for the excellent microwave absorption abilities. In detail, the minimum RL value is -51.3 dB at 15.2 GHz and the maximum effective absorption frequency width (< -10 dB) is 5.1 GHz both with 1.8 mm. Our work may be helpful for the exploitation of lightweight microwave absorbers in near future.

Method

Materials. All chemicals and reagents are supplied by business supporters and they are all without pretreated. These chemicals are polyacrylonitrile (PAN, $M_w = 150\,000$) and polyvinylpyrrolidone (PVP, $M_w = 5\,800$). *N,N*-dimethylformamide (DMF) is needed as well.

Synthesis of carbon nanofibers. Carbon nanofibers were obtained by electrospinning technology and following high-temperature carbonization. First, 0.5 g of PAN was added into 5 mL DMF with continuous magnetic stirring. Then, a certain amount of PVP was also introduced to this system with stirring for 24 h to achieve a transparent and syrupy liquid. The mass ratio of PAN and PVP is 7:3, 6:4 and 5:5, respectively. The precursor nanofibers are called PAN/PVP-7/3, PAN/PVP-6/4 and PAN/PVP-5/5, respectively. Second, this liquid was sucked into a 5 mL plastic syringe equipped with a stainless needle. The next process was the electrospinning. Specifically, the voltage parameters were 20 kV, the collection distance was 15 cm and the pushing speed was 0.5 mL/h. After that, the precursor PAN/PVP nanofibers were dried in a vacuum oven for a day and the PAN/PVP nanofibers were calcined at 800 °C for 3 h surrounded with N_2 atmosphere. Herein, the average rate was of 2 °C per minute. And the carbon nanofibers are marked as PVP (214), PVP (333) and PVP (500), respectively. When these PAN/PVP nanofibers were heated at 200 °C, 400 °C and 600 °C, these samples are named as PVP (214-200), PVP (333-200), PVP (500-200), PVP (214-400), PVP (333-400), PVP (500-400), PVP (214-600), PVP (333-600) and PVP (500-600), respectively.

Characterization. The crystal structure was measured by X-ray diffraction (XRD) under Cu $K\alpha$ radiation. The SEM (Hitachi-S4800) as well as TEM (Tecnai G2 F30) were used to observe the microtopography of these nanofibers. A vector network analyzer (Agilent, N5244A) was applied to test the electromagnetic parameters in the range of 2–18 GHz. The samples (20% filler ratio) and paraffin (80% filler ratio) were crushed into a cylinder. The inner diameter and the outer diameter were 3.0 mm and 7.0 mm. When changing the filler ratio, the samples (30%, 40% and 50% filler ratio) are called as PVP (214, 30), PVP (333, 30), PVP (500, 30), PVP (214, 40), PVP (333, 40), PVP (500, 40), PVP (214, 50), PVP (333, 50) and PVP (500, 50), respectively.

References

- You, W. B., She, W., Liu, Z. W., Bi, H. & Che, R. C. High-temperature annealing of an iron microplate with excellent microwave absorption performance and its direct micromagnetic analysis by electron holography and Lorentz microscopy. *J. Mater. Chem. C* **5**, 6047–6053 (2017).
- Quan, B. *et al.* Laminated graphene oxide-supported high-efficiency microwave absorber fabricated by an *in situ* growth approach. *Carbon* **129**, 310–320 (2018).
- Zhang, C. *et al.* Microwave absorption properties of CoS_2 nanocrystals embedded into reduced graphene oxide. *ACS Appl. Mater. Interfaces* **9**, 28868–28875 (2017).
- Zhou, J. *et al.* Facile synthesis of three-dimensional lightweight nitrogen-doped graphene aerogel with excellent electromagnetic wave absorption properties. *J. Mater. Sci.* **53**, 4067–4077 (2018).
- Liu, W. *et al.* Metal-organic-frameworks derived porous carbon-wrapped Ni composites with optimized impedance matching as excellent lightweight electromagnetic wave absorber. *Chemical Engineering Journal* **313**, 734–744 (2017).
- Cheng, Y. H. *et al.* Strong and thermostable SiC nanowires/graphene aerogel with enhanced hydrophobicity and electromagnetic wave absorption property. *Applied Surface Science* **448**, 138–144 (2018).
- Zhao, X. X. *et al.* High rate and long cycle life porous carbon nanofiber paper anodes for potassium-ion batteries. *J. Mater. Chem. A* **5**, 19237–19244 (2017).
- Xu, G. Y. *et al.* Porous nitrogen and phosphorus co-doped carbon nanofiber networks for high performance electrical double layer capacitors. *J. Mater. Chem. A* **3**, 23268–23273 (2015).
- Davis, T. A., Patberg, S. M., Sargent, L. M., Stefaniak, A. B. & Holland, L. A. Capillary electrophoresis analysis of affinity to assess carboxylation of multi-walled carbon nanotubes. *Analytica Chimica Acta* **1027**, 149–157 (2018).
- Jeon, H. *et al.* Facile and fast microwave-assisted fabrication of activated and porous carbon cloth composites with graphene and MnO_2 for flexible asymmetric supercapacitors. *Electrochimica Acta* **280**, 9–16 (2018).
- Li, G., Xie, T. S., Yang, S. L., Jin, J. H. & Jiang, J. M. Microwave absorption enhancement of porous carbon fibers compared with carbon nanofibers. *J. Phys. Chem. C* **116**, 9196–9201 (2012).

12. Wan, G. P. *et al.* Preparation and microwave absorption properties of uniform TiO₂@C core-shell nanocrystals. *RSC Adv.* **5**, 77443–77448 (2015).
13. Wang, F. Y. *et al.* *Carbon.* **134**, 264–273 (2018).
14. Hou, Z. R. *et al.* Microwave absorption properties of single- and double-layer absorbers based on electrospun nickel-zinc spinel ferrite and carbon nanofibers. *Journal of Materials Science: Materials in Electronics.* **14**, 12258–12268 (2018).
15. Liu, H. H. *et al.* *In situ* preparation of cobalt nanoparticles decorated in N-doped carbon nanofibers as excellent electromagnetic wave absorbers. *ACS Appl. Mater. Interfaces.* **10**, 22591–22601 (2018).
16. Liu, L., He, P. G., Zhou, K. C. & Chen, T. F. Microwave absorption properties of helical carbon nanofibers-coated carbon fibers. *AIP Advances.* **3**, 082112 (2013).
17. Zhang, T. *et al.* Porous-carbon-nanotube decorated carbon nanofibers with effective microwave absorption properties. *Nanotechnology.* **28**, 355708 (2017).
18. Chu, Z. Y., Cheng, H. F., Xie, W. & Sun, L. K. Effects of diameter and hollow structure on the microwave absorption properties of short carbon fibers. *Ceramics International.* **38**, 4867–4873 (2012).
19. Lv, J. *et al.* Structural and Carbonized design of 1D FeNi/C nanofibers with conductive network to optimize electromagnetic parameters and absorption abilities. *ACS Sustainable Chem. Eng.* **6**, 7239–7249 (2018).
20. An, G. H., Lee, D. Y. & Ahn, H. J. Tunneled mesoporous carbon nanofibers with embedded ZnO nanoparticles for ultrafast lithium storage. *ACS Appl. Mater. Interfaces.* **9**, 12478–12485 (2017).
21. Yang, Y., Li, X., Shen, L. D., Wang, X. F. & Benjamin, S. H. A durable thin-film nanofibrous composite nanofiltration membrane prepared by interfacial polymerization on a double-layer nanofibrous scaffold. *RSC Adv.* **7**, 18001–18013 (2017).
22. Mohsenpour, S. & Khosravianian, S. Influence of additives on the morphology of PVDF membranes based on phase diagram: Thermodynamic and experimental study. *J. Appl. Polym. Sci.* **1002**, 46225 (2018).
23. Liu, X. F. *et al.* Tuning microwave absorption properties by hybridizing heterogeneous components for core@shell structural Fe@SiC flakes. *Journal of Magnetism and Magnetic Materials.* **462**, 46–52 (2018).
24. Dong, S. *et al.* Nitrogen content dependent microwave absorption property of nitrogen-doped SiC materials annealed in N₂: opposing trends for microparticles and nanowires. *Journal of Alloys and Compounds.* **758**, 256–267 (2018).
25. Qiao, M. T. *et al.* Application of yolk-shell Fe₃O₄@N-doped carbon nanochains as highly effective microwave-absorption material. *Nano Res.* **11**, 1500–1519 (2018).
26. Mordina, B., Kumar, R., Tiwari, R. K., Setua, D. K. & Sharma, A. Fe₃O₄ nanoparticles embedded hollow mesoporous carbon nanofibers and polydimethylsiloxane-based nanocomposites as efficient microwave absorber. *J. Phys. Chem. C.* **121**, 7810–7820 (2017).
27. Li, N. *et al.* Enhanced microwave absorption performance of coated carbon nanotubes by optimizing the Fe₃O₄ nanocoating structure. *ACS Appl. Mater. Interfaces.* **9**, 2973–2983 (2017).
28. Yin, Y. C., Liu, X. F., Wei, X. J., Yu, R. & Shui, J. L. Porous CNTs/Co composite derived from zeolitic imidazolate framework: a lightweight, ultrathin, and highly efficient electromagnetic wave absorber. *ACS Appl. Mater. Interfaces.* **8**, 34686–34698 (2016).
29. Wang, W. & Cao, M. H. Ni₃Sn₂ alloy nanocrystals encapsulated within electrospun carbon nanofibers for enhanced microwave absorption performance. *Materials Chemistry and Physics.* **177**, 198–205 (2016).
30. Zhang, X. J. *et al.* Enhanced microwave absorption property of reduced graphene oxide (RGO)-MnFe₂O₄ nanocomposites and polyvinylidene fluoride. *ACS Appl. Mater. Interfaces.* **6**, 7471–7478 (2014).
31. Lv, H. L. *et al.* A voltage-boosting strategy enabling a low-frequency, flexible electromagnetic wave absorption device. *Adv. Mater.* **1706343**, 1–8 (2018).
32. Zhu, L. Y., Zeng, X. J., Chen, M. & Yu, R. H. Controllable permittivity in 3D Fe₃O₄/CNTs network for remarkable microwave absorption performances. *RSC Adv.* **7**, 26801–26808 (2017).
33. Xing, H. L. *et al.* Excellent microwave absorption properties of Fe ion-doped SnO₂/multi-walled carbon nanotube composites. *RSC Adv.* **6**, 41656–41664 (2016).
34. Zhang, Z. C. *et al.* Electrospinning and microwave absorption of polyaniline/polyacrylonitrile/multiwalled carbon nanotubes nanocomposite fibers. *Fibers and Polymers.* **11**, 2290–2296 (2014).
35. Lv, X. *et al.* Preparation and electromagnetic properties of carbon nanofiber/epoxy composites. *Journal of Macromolecular Science, Part B: Physics.* **49**, 355–365 (2010).

Acknowledgements

We are very thankful for financial support from the National Nature Science Foundation of China (No. 11575085), the Aeronautics Science Foundation of China (2017ZF52066), Qing Lan Project, Six talent peaks project in Jiangsu Province (No. XCL-035), Jiangsu 333 talent project, and the Open Research Fund of Jiangsu Provincial Key Laboratory for Nanotechnology of Nanjing University.

Author Contributions

Baoshan Zhang designed this nanofibers material structure. Jing Lv performed the experiments. Weihua Gu and Xiaoqing Cui collected the experimental data. Guangbin Ji and Sisi Dai measured the electromagnetic parameters. Baoshan Zhang provided insightful discussions for the dielectric loss. Jing Lv organized the manuscript. All authors contributed to preparing the manuscript.

Additional Information

Competing Interests: The authors declare no competing interests.

Publisher's note: Springer Nature remains neutral with regard to jurisdictional claims in published maps and institutional affiliations.



Open Access This article is licensed under a Creative Commons Attribution 4.0 International License, which permits use, sharing, adaptation, distribution and reproduction in any medium or format, as long as you give appropriate credit to the original author(s) and the source, provide a link to the Creative Commons license, and indicate if changes were made. The images or other third party material in this article are included in the article's Creative Commons license, unless indicated otherwise in a credit line to the material. If material is not included in the article's Creative Commons license and your intended use is not permitted by statutory regulation or exceeds the permitted use, you will need to obtain permission directly from the copyright holder. To view a copy of this license, visit <http://creativecommons.org/licenses/by/4.0/>.

© The Author(s) 2019